energies

MDPI

Article

How Much Can Small-Scale Wind Energy Production Contribute to Energy Supply in Cities? A Case Study of Berlin

Alina Wilke [1,*], Zhiwei Shen [2] and Matthias Ritter [2]

[1] Department of Macroeconomic Theory and Policy, Schumpeter School of Business and Economics, Bergische Universität Wuppertal, 42119 Wuppertal, Germany
[2] Department of Agricultural Economics, Faculty of Life Sciences, Humboldt-Universität zu Berlin, 10117 Berlin, Germany; shenzhiw@agrar.hu-berlin.de (Z.S.); matthias.ritter@agrar.hu-berlin.de (M.R.)
* Correspondence: wilke@wiwi.uni-wuppertal.de; Tel.: +49-202-439-3174

Abstract: In light of the global effort to limit the temperature rise, many cities have undertaken initiatives to become climate-neutral, making decentralized urban energy production more relevant. This paper addresses the potential of urban wind energy production with small wind turbines, using Berlin as an example. A complete framework from data selection to economic feasibility is constructed to enable the empirical assessment of wind energy for individual buildings and Berlin as a whole. Based on a detailed dataset of all buildings and hourly wind speed on a 1 km^2 grid, the results show that multiple turbines on suitable buildings can significantly contribute to households' energy consumption but fall short of covering the full demand. For individual households, our economic evaluation strongly recommends the self-consumption of the produced electricity. The findings suggest that while the use of small wind turbines should be continuously encouraged, exploring other renewable resources or combination of wind and photovoltaic energy in the urban environment remains important.

Keywords: renewable energy; urban wind energy; energy transition; wind potential assessment

Citation: Wilke, A.; Shen, Z.; Ritter, M. How Much Can Small-Scale Wind Energy Production Contribute to Energy Supply in Cities? A Case Study of Berlin. *Energies* **2021**, *14*, 5523. https://doi.org/10.3390/en14175523

Academic Editors: Davor Mikulić and Damira Keček

Received: 22 July 2021
Accepted: 1 September 2021
Published: 4 September 2021

1. Introduction

The COVID-19 pandemic caused global energy demand to hit a historic decrease of 4% in 2020, the largest decrease since World War II [1]. Despite this, it is predicted to surpass pre-COVID-19 levels in 2021, maintaining its continuous growth path of the previous years [1]. Emerging markets, such as the People's Republic of China, are contributing to this increase [1]. Electricity demand has even experienced its fastest growth of the past 10 years in 2021 [1]. Growing energy consumption increases the amount of greenhouse gas emissions since most of the global energy supply is still derived through burning fossil fuels [2]. Oil made up 30.9% of global primary energy supply in 2019, followed by coal with 26.8%. Renewable energy consumption on the other hand decreases CO_2 emission levels [3,4] and the replacement of fossil energy by renewable energy is key to reaching the ambitious objectives to tackle global warming. There have been numerous definitions of objectives of governments and international organizations to increase renewables consumption and therewith decrease CO_2 emissions to tackle climate warming. In the Paris Agreement, 195 State Parties committed to increase the global efforts to limit the temperature rise below two degrees Celsius above the preindustrial level [5]. The member states of the European Union even legally committed to reduce greenhouse gas emissions by 55% by 2030 (as compared to 1990 levels) through the European Green Deal [6].

Wind and solar power are the renewables that for now contribute most to the energy transition, showing the largest growth rate since the 1980s, followed by biofuels [1]. Yet, small wind energy makes up such a small part of the global renewable energy mix, that its share is normally not even considered in reports on global renewable energy. To strongly decrease CO_2 emissions in the near future, all potential installation sites should be

used for renewable energy production. There could still be scope to increase renewable energy supply by discovering urban production sites, especially since urbanization and population growth positively affect CO_2 emission levels [3,7], making cities emission hotspots. Regional energy production also decreases the transmission losses that electricity (through which renewable energy is most commonly carried out) suffers from long-distance transportation [8,9]. Increasing regional efforts to produce renewable energies could nudge the process of Schumpeterian creative destruction in energy markets. Inefficient, oligopolistic energy markets might decrease since many regions will be able to produce a large part of their energy demand themselves [9].

Small wind turbines (SWT) pose a promising opportunity to take renewable energy to a regional level and to benefit from existing high building structures, such as towers or high-rise buildings. However, SWT are still considered less efficient than large wind turbines [8,10,11]; on the one hand this is due to the state of their technical development, on the other hand it is due to insufficient investigation of wind conditions at suitable installation locations, such as the built environment [12]. Still, growing research on the technical design of SWT [13–15], as well as on wind conditions in the urban environment [16], indicates potential for a more extensive application of SWT. They can often be installed without a building permit, produce low noise emissions, and have also a high degree of technical reliability [17–20].

This paper sheds light on the potential of urban wind energy production by simulating the installation of SWT on each building above 10 m of height in the city of Berlin. This is done by combining narrow wind grid data, 3-D building data and the power curve of an exemplary, roof-mounted turbine. Additionally, we assess the economic feasibility of the turbine installation for an individual investor.

The following research questions will be addressed:

1. *How much energy could be produced in Berlin through the installation of roof-mounted turbines?*
2. *By how much could CO_2 emissions be reduced in Berlin?*
3. *By how much would the installation of a single roof-mounted SWT result in a profit or loss in Berlin?*

Hence, the contribution of this paper is threefold: Firstly, it provides a solid framework to assess the potential of wind energy in the urban environment. The approach could also be applied to other cities. Secondly, it analyzes the economic feasibility of wind turbine installation on the household level. Thirdly, it provides a dataset of all buildings in Berlin, including their coordinates, roof-surface, building height and a unique ID, which is available upon request from the corresponding author. The dataset was derived from the processing and expansion of the initial building dataset. We consider the wake effect of surrounding buildings or nearby installed turbines through a sensitivity analysis. The urban wind energy potential of Berlin is compared with other energy sources such as large wind turbines onshore and offshore or photovoltaic.

Whereas the focus of the paper is narrowed to the use of SWT, it does not claim that this is the only or the best option. Using the building rooftops for photovoltaic (maybe in combination with SWT) or producing energy with large turbines outside of Berlin might be more feasible.

The remainder of the paper is organized as follows: Section 2 presents the methodology, particularly the derivation of the wind energy potential per building and the background for the economic evaluation; Section 3 provides details about study region and data (wind speeds, buildings, and reference turbine); Section 4 presents the results at the city- and household-level; in Section 5 the results are discussed; and Section 6 concludes.

2. Methods

2.1. Derivation of Wind Energy Potential

For the assessment of potential energy production with a rooftop installed SWT, it is necessary to work with three datasets, namely wind data, building height data, and

a turbine power curve. Figure 1 shows the flow diagram of the applied methodology. Datasets are displayed in a rhombus shape, with blue rhombuses representing the initial datasets and grey rhombuses representing datasets that result from the analysis. White rectangles distinguish processes.

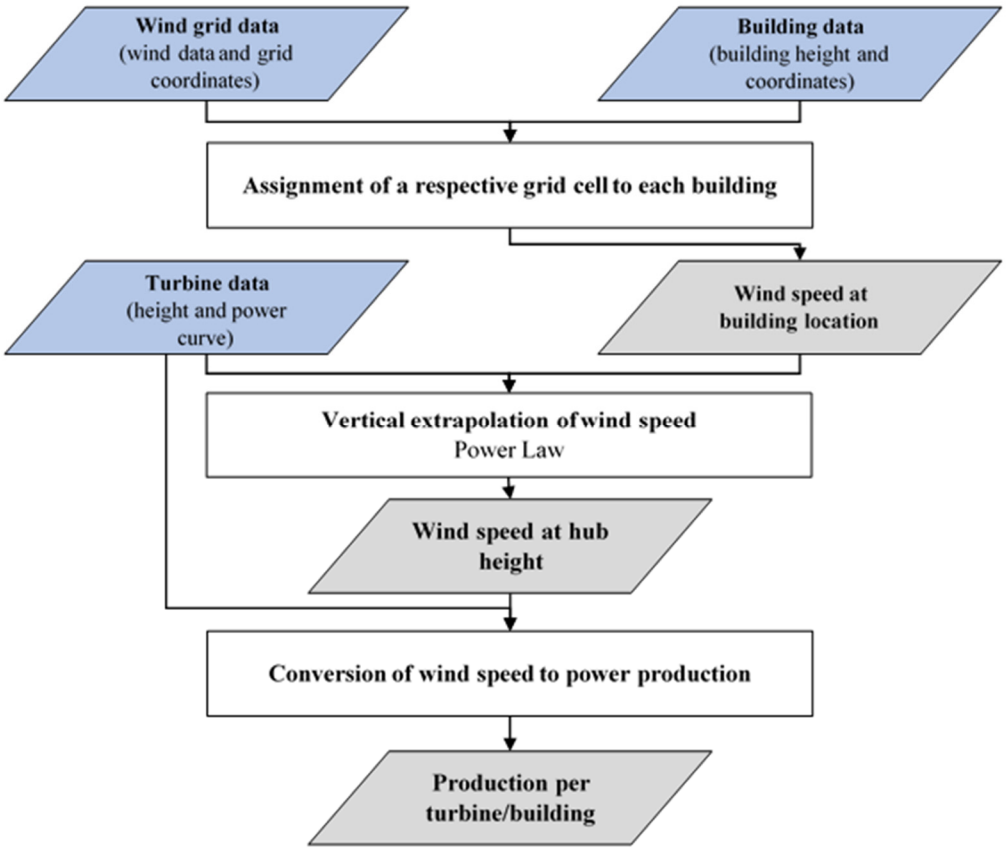

Figure 1. Flow diagram of methodology. Source: Own representation.

Due to the unique characteristics of urban wind flows, the most accurate wind data is obtained when directly measured at the point of interest, i.e., at the hub height of the roof-mounted turbine. This, however, would be extremely time-consuming and costly, especially at a larger scale. The alternative of taking measurements at a few buildings and interpolating these measurements to surrounding buildings would not yield reliable results either since microclimates inside cities vary widely due to turbulences and the off flow of air [21,22].

A convenient solution is the usage of reanalysis wind data provided in a grid format. Wind measurements for grid datasets are taken at meteorological stations at a standardized height, which are typically located at an open field with few obstacles. The provider of the grid dataset performs a horizontal interpolation of the station data to the grid points. To obtain wind measurements at the hub height of a roof-mounted turbine, the grid data must further be horizontally interpolated to the building's exact location and vertically extrapolated to the hub height of the turbine. If wind data is provided in a very narrow grid, further interpolation can be avoided since it would be prone to errors and imprecision, especially if it is not performed by specialists. As an approximation, buildings can be assigned to their closest grid point before the wind speed is vertically extrapolated to the hub height of the roof-mounted turbine.

In the literature, vertical extrapolation of wind speed is typically performed with either of two mathematical approaches, namely the power law and the logarithmic law. The power law is defined as:

$$v_i = v_r * \left(\frac{z_i}{z_r}\right)^{\alpha}, \quad (1)$$

with wind speed v_i at turbine height z_i, reference wind speed v_r at reference height z_r, and wind shear coefficient (WSC) α. The power law yields an "*accurate and better representation of wind speed profiles*" (Gualtieri and Secci 2012, p. 183) [23] than the logarithmic model, at least under unstable and neutral conditions [24,25]. It is valid for heights up to 150–200 m above ground level [23]. Furthermore, it requires only one unknown coefficient, namely WSC α.

The WSC α assesses the vertical wind shear profile, which describes changes in wind velocities with respect to height [26]. If wind measurements at only one height are available, the WSC can be approximated as 1/7 according to the power law "rule of thumb" [23,27]. However, the WSC was found to strongly depend on variation in turbulence intensities [24,25,28]. Since turbulence is greatly affected by surface roughness, the "rule of thumb" might be an imprecise approximation, especially in cities. It is, however, possible to derive a reliable general WSC when surface roughness is considered [24]. The roughness length reflects land features that cause turbulence [24,25,29]. This analysis deals with wind patterns in the relatively closed urban climate Therefore, a general value for the roughness length is determined and a general WSC will be derived for the whole study region.

Gualtieri and Secci (2011) [24] find that the combination of vertical extrapolation using the power law together with the WSC calculation proposed by Smedman-Högström and Höström (1978) [30] yields the overall best performance and provides a "*definitely reliable method*" for calculating "*initial estimates of wind potential at hub height*" (Gualtieri and Secci 2011, p. 2203f). Therefore, we apply formula and parameters proposed for unstable and slightly unstable conditions by Smedman-Högström and Höström (1978) [30] as displayed in Equation (2).

$$\alpha = 0.18 + 0.13\ln(z_0) + 0.03[\ln(z_0)]^2 \quad (2)$$

Here, z_0 denotes the roughness length, which reflects the degree of wind-breaking obstacles [8,21,22] and is defined as approximately one-tenth of the average height of surface roughness elements (buildings, trees, etc.). The WMO (2017) [31] published a list of roughness length parameters for different terrains, specifying that z_0 is equal to 1 m in suburban terrains and larger or equal to two meters in city centers with high- and low-rise buildings. Counihan (1975) [25] concludes that roughness lengths of two to three meters are typical for urban areas. Manwell et al. (2009) [26] provide a list of roughness lengths according to the type of terrain, defining z_0 equal to approximately three meters in city centers with tall buildings and 1.5 m in suburbs. Following the literature, in this analysis an approximate roughness length of two meters will be used for our main calculation since the focus lies in cities that consist of both city centers and suburban areas. This yields a WSC of approximately 0.28, which lies in the range of typical WSCs for urban and rough terrains, 0.21–0.40, found by Counihan (1975) [25]. To explore the sensitivity of our results to the roughness length, we additionally derive the expected annual electricity production throughout Berlin assuming z_0 = 1.5 or z_0 = 3.

After vertically extrapolating wind speeds to the hub heights of the rooftop-installed turbines, the conversion to energy output is conducted via the power curve, which is typically provided by the turbine manufacturer.

2.2. Economic Evaluation

In addition to the power production capacity evaluation, we want to create insights into the economic trade-offs of the installation of a single VAWT on an average building in Berlin. The levelized costs of electricity (LCOE), which are commonly used to compare

investments in renewable energy projects [32–34], are applied in this analysis. The LCOE measure the net present costs of electricity production over a turbine's lifetime. Breaking down to one specific unit of energy it can be regarded as the minimum price at which this unit of electricity must be sold in order to not make losses over the lifetime of the turbine [35]. The LCOE are calculated based on Equation (3),

$$LCOE = \frac{C_0 + \sum_{t=1}^{N} \frac{o_t}{(1+r_d)^t}}{\sum_{t=1}^{N} \frac{E_t}{(1+r_d)^t}}, \quad (3)$$

where: C_0 is the initial investment required for the installation of the reference turbine, i.e., purchase costs and installation costs (15% of the purchase price, following MWEA (2005) [36]); o_t are the cash outflows in period t; and r_d is the discount rate. N is the amount of years with guaranteed feed-in tariffs under the EEG regime, namely 20 years, following the approach of Grieser et al. (2015) [10]. Operative outflows are assumed to consist of annual operation costs, maintenance costs, and debt service. The costs for the initial investment C_0 can be debt-financed, equity-financed, or a mixture of both. In this analysis, we consider the first two possibilities, while including a sensitivity analysis for the costs of equity (CoE).

This results in four different LCOE-scenarios: debt-financing, equity-financing with low CoE, equity-financing with medium CoE, and equity-financing with high CoE.

3. Study Region and Data

This chapter provides an overview of the study region Berlin, including the legal framework for the SWT installation and insights on wind conditions in the city. Furthermore, the applied data is introduced, namely the wind dataset, the building dataset, and the power curve of the reference turbine.

3.1. Study Region Berlin

Berlin lies in the northeast of Germany at 52°31′ N, 13°24′ E. The city state of Berlin has the highest population density among German municipalities, and 55.3% of its area are settled with buildings [37]. Besides a high surface roughness due to the density of buildings, Berlin is mainly flat topographically. The highest elevation, *Großer Müggelberg*, is just 115 m above ground-level [21]. Natural ground roughness is negligible, so the focus of this study can be laid on human-shaped surface roughness, especially buildings.

The legal basis for all kinds of construction projects, in our case small, roof-mounted turbines below 30 m in height, is the Federal State Building Order of Berlin [38]. It exempts nearly all construction below this height from the requirement of a legal building permit (§62, BauO Bln); however, this exemption does not mean that SWT can be constructed everywhere without having to comply with other regulations. If SWT are classified as an ancillary facility (*Nebenanlage*), they can be built in any construction area, but they must comply with specific requirements regarding the consumption of the produced electricity and visual disturbance to the supporting building. Noise emission, vibration, and shadowing that could affect the neighborhood must also be considered [18].

3.2. Wind Data

The representative Test Reference Year (TRY), which was constructed by the German Meteorological Service (*Deutscher Wetterdienst*, DWD) and the German Federal Office for Building and Regional Planning (*Bundesamt für Bauwesen und Raumordnung*, BBR) in 2017 [39] is used to assess wind conditions in Berlin. It provides wind speed and direction in a 1 km^2 grid resolution throughout Germany and includes hourly wind measurements from 1995 to 2012, measured at 10 m above the ground [40]. For this study, the mean climate scenario for 2015 will be used (hereafter, TRY 2015).

Figure 2 shows the average hourly wind speeds per grid cell in the TRY 2015 for Berlin. As expected, we observe low wind speeds in the city center where the density of high

buildings does not allow for the wind to pick up much speed. The highest wind speeds are observed in the outskirts of the city, namely in the southwest, southeast, and the northern areas of Berlin. These areas lie inside large stretches of water or moor, so the wind can blow undisturbed and reach higher velocities.

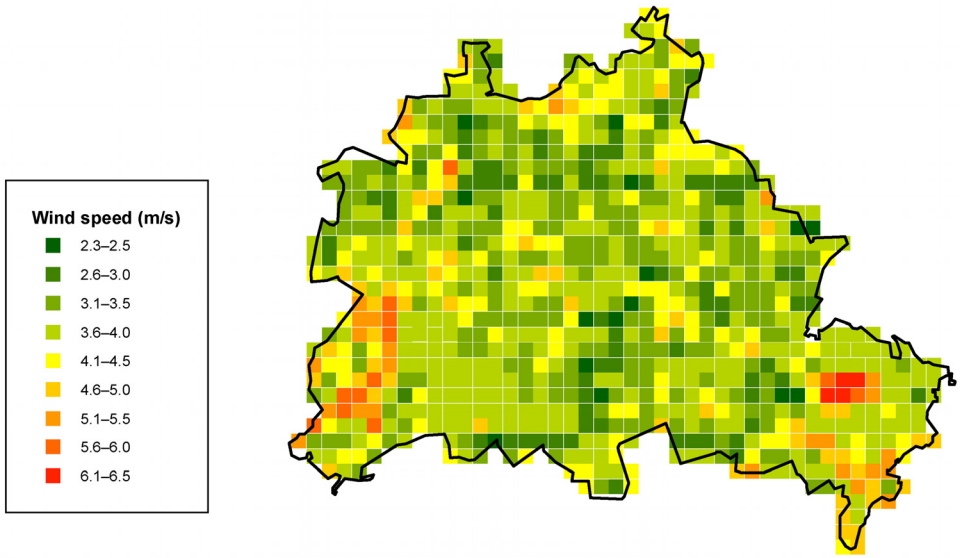

Figure 2. Average hourly wind speed per grid cell (1 km^2) in Berlin. Source: Own representation of TRY 2015 [39].

The average wind speed over all grid cells in the TRY 2015 is 3.7 m/s. Figure 3 displays the distribution of wind speeds in TRY 2015 with a fitted Weibull distribution, as well as the corresponding wind rose. The maximum wind speed in the distribution is 22.6 m/s; however, for the sake of a clear visual presentation, extreme and rare wind speeds above 15 m/s are excluded from the shown histogram.

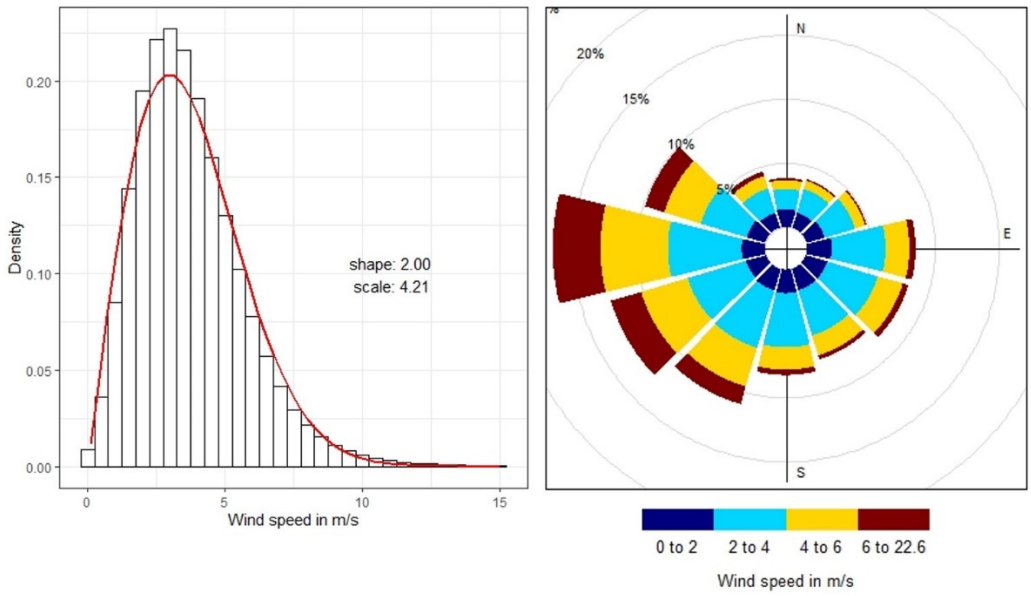

Figure 3. Histogram with fitted Weibull distribution (**left**) and wind rose (**right**) for TRY 2015. Source: Own representation of TRY 2015 [39].

Lun and Lam (2000) [41] found that the long-term shape parameter of the Weibull distribution varies from 1.63 in an urban area to 2.03 in an offshore environment. The

Weibull distribution of TRY 2015 has a shape parameter of 2.00, which is close to that at an offshore environment and indicates relatively few turbulences. This can mostly be explained by the fact that the TRY 2015 includes average data over 17 years. The main wind directions in Berlin are west and southwest, whereas north and northeast are least frequent.

The DWD also provides historic wind speed measurements for many meteorological stations in Germany. This allows us to perform a validity check of the grid dataset by comparing the data of the 1 km^2 square of TRY 2015 with hourly wind speed measurements from the meteorological station Berlin-Tempelhof in 2015 [42]. Figure 4 shows the histograms of historic wind records for Berlin-Tempelhof in 2015 (left) and the TRY 2015 data in the Tempelhof grid cell (right). The distributions of wind speed are very similar, but the TRY 2015 shows more outliers around its mean, which indicates more turbulent wind flows. In addition, the shape parameter of the TRY 2015 at the Tempelhof grid cell is slightly lower than that of the real observations from 2015, which is a further signal for more turbulent wind flows. Although there are more turbulences in our dataset than measured in 2015, the results of the direct comparison increase the confidence in the TRY 2015 dataset.

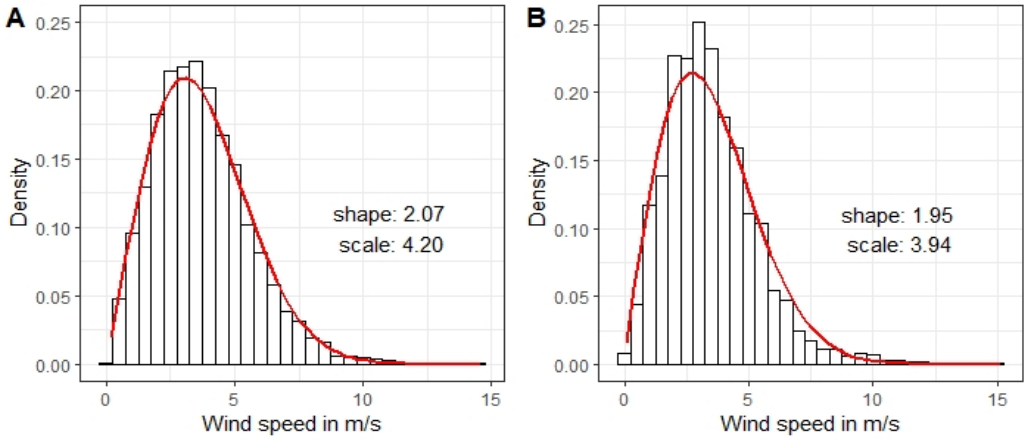

Figure 4. Histograms and fitted Weibull distributions for (**A**) historical observations in Tempelhof meteorological station in 2015 and (**B**) in the TRY 2015 Tempelhof grid cell. Source: Own representation of TRY 2015 [39] and hourly wind speed at Berlin-Tempelhof in 2015 [42].

3.3. Building Data

The building dataset is provided by the Berlin Senate Administration for Urban Development and Housing (*Senatsverwaltung für Stadtentwicklung und Wohnen*) through a 3D Building Model in Level of Detail 1 (LoD1), i.e., all buildings are modelled as blocks without details about their roofs [43]. The applied dataset reflects the situation on the 28th of March 2018.

Each building is assigned a unique coordinate. The raw building dataset consists of 632,821 data points. Buildings below 10 m in height are omitted in this analysis since wind in the urban environment reduces sharply with decreasing height above ground due to obstructions. Hence, buildings below 10 m located in an urban area like Berlin are unlikely to yield profitable outcomes. A height of 10 m also corresponds to the height usually used for wind measurements at weather stations and for the TRY 2015. Additionally, buildings with a roof surface area below 2 m^2 are ignored because most roof-installed turbines need at least this area for their base structure. The remaining building dataset entering the analysis contains 94,992 data points.

Figure 5 depicts the distribution of the buildings over the grid cells in Berlin. As expected, the number of buildings is higher in the densely populated areas of Berlin, such as the center, west, and south. Blank cells indicate that there is no suitable building, often because of lakes or forests. The strikingly red cell with over 1000 buildings contains the Horseshoe Estate (*Hufeisensiedlung*), which consists of 679 family homes that are slightly

higher than 10 m. For further information on the characteristics of the building dataset and the transformation process that was performed to prepare dataset for this analysis, see Appendix A. To structure the analysis and generalize the results, we divide the buildings into four categories according to their height (see Table 1). The vast majority of buildings in our dataset have a height between 10 and 30 m. Very few buildings reach a height above 40 m.

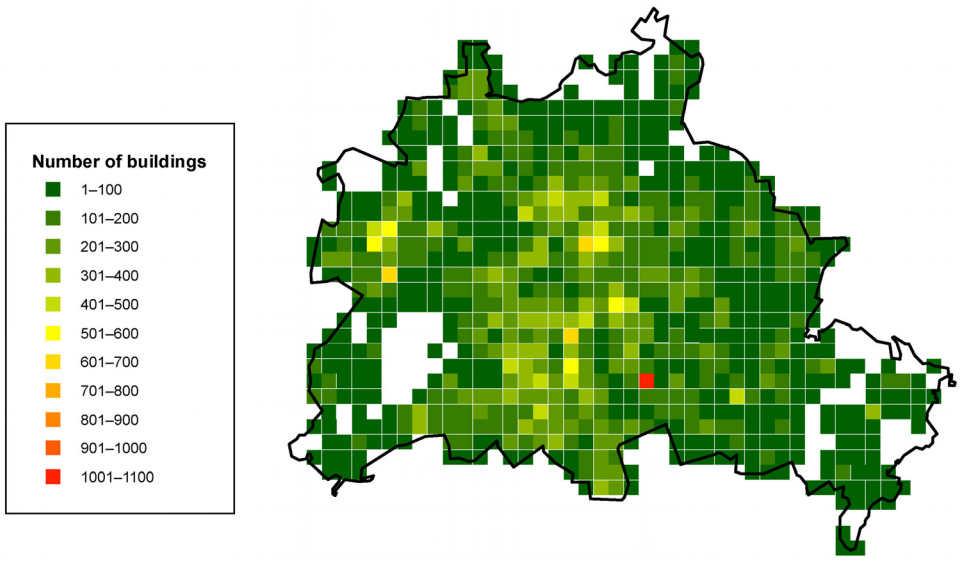

Figure 5. Number of buildings higher than 10 m, with minimum roof-area of 2 m^2, per grid cell. Source: Own representation of Senatsverwaltung für Stadtentwicklung und Wohnen Berlin, 2015 [43].

Table 1. Building categories (BCs) and corresponding number of buildings.

Building Category	Building Height	Number of Buildings	Share
BC 1	10 m–20 m	76,109	80.12%
BC 2	20 m–30 m	17,025	17.92%
BC 3	30 m–40 m	1546	1.63%
BC 4	>40 m	312	0.32%
Total		94,992	100.00%

Source: Own representation of Senatsverwaltung für Stadtentwicklung und Wohnen Berlin, 2015 [43].

3.4. Reference Turbine

There are two types of wind turbines that are commonly used in the urban environment: horizontal axis wind turbines (HAWT) have a rotor shaft that lies horizontally to the wind and must be pointed at it; vertical axis wind turbines (VAWT) have a rotor shaft that is situated perpendicular to the wind [17,18]. VAWT are especially suitable in urban environments because—in contrast to HAWT—they rotate independently of the wind direction, so they do not have to point directly at the wind to work effectively. They might even benefit from turbulences, which are typical in urban areas. In addition, VAWT can be installed closer to the ground due to their low noise emissions. Finally, VAWT have a low impact on birds and the generator and gearbox can be installed at the ground level, which lowers the average maintenance cost [17–19].

For our case study, we use the Skyline SL-30 turbine from the Italian manufacturer En-Eco with an H-Darrieus rotor (see product sheet [44]). The same turbine was also used in the performance analysis by Bortolini et al. [11] from where we took the purchasing price of EUR 3,840. The turbine is technically suitable for rooftop installation and does not require a building permit. However, in practice, when a turbine is installed, effects on neighbors and a structural analysis of the building should be considered.

The technical data of the Skyline SL-30 turbine and its power curve are depicted in Table 2 and Figure 6. The rated power is the production capacity of the turbine at the rated wind speed. The maximum power indicates the power output that can be maximally reached without breaking the turbine. If the wind speed further increases, the turbine switches off. The cut-off speed indicates the speed at which this happens. The hub height indicates the height from the bottom of the turbine to the rotor, without the blades.

Table 2. Technical data of reference turbine Skyline SL-30.

Skyline SL-30	
Manufacturer	En-Eco
Rated wind speed (m/s)	12
Rated power (kW)	3
Maximum power (kW)	3.6
Cut-in speed (m/s)	3
Cut-off speed (m/s)	16
Hub height (m)	8
Total weight (kg)	258

Source: Own representation of data from the manufacturer En-Eco [44].

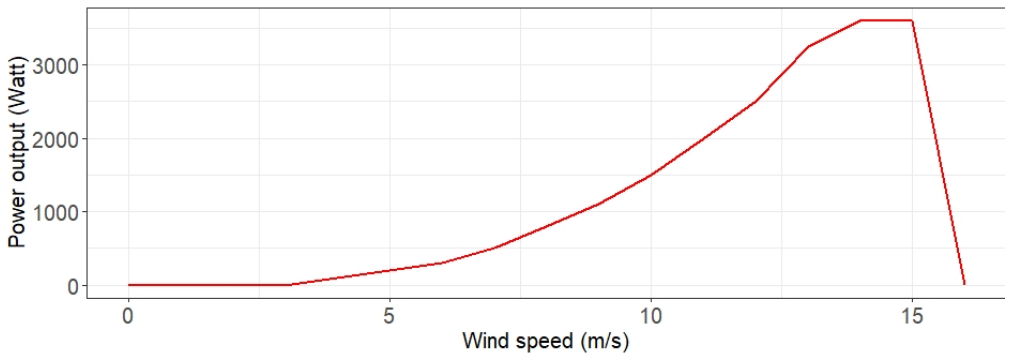

Figure 6. Power curve of reference turbine Skyline SL-30. Source: own representation based on information of the manufacturer [44].

Considering the mean wind speed of TRY 2015, the typical wind speed in Berlin amounts to 3.5 m/s with a mean variation of 1.88 m/s at 10 m height. With the turbine's cut-in wind speed of 3 m/s lying below this mean wind speed and turbines being installed only on buildings with a minimum height of 10 m, the average wind speed at the hub height clearly outreaches the cut-in wind speed. The maximum wind speed in the TRY 2015 was approximately 22 m/s at 10 m height; however, wind speeds above the cut-off speed of 16 m/s were reached for just 0.014% of the total hours in the TRY 2015 dataset. The turbine should therefore also deal well with the range of wind speeds in Berlin.

4. Results

4.1. City-Level

4.1.1. Scenarios—Varying the Number of Turbines per Building

Scenario 1 refers to our base scenario, namely the installation of one turbine of each eligible building. Table 3 displays the accumulated annual energy production and mean wind speeds at the hub height for Scenario 1.

Throughout Berlin, 207,281 MWh of energy could be produced per year if one chosen reference turbine was installed on all buildings that are at least 10 m in height with a minimum roof surface of 2 m^2, corresponding to 94,992 turbines in total.

Distinguishing the results for the different building categories shows that the largest share (75%) is contributed by small buildings with a height between 10 m and 20 m, which is caused by the fact that most buildings in the dataset belong to that height range. Only 312 buildings are higher than 40 m, but there are 76,109 buildings between 10 m and 20 m.

Table 3. Number of potentially installed turbines, average wind speed at hub height, average annual energy production per turbine, and accumulated annual energy production for Berlin by building categories (BCs).

	Number of Turbines	Average Wind Speed, Extrapolated (m/s)	Average Energy Production Per Turbine (MWh)	Sum of Energy Production (MWh)	Share of Total Energy Production
BC 1 (10–20 m)	76,109	4.4	2.05	156,232	75.37%
BC 2 (20–30 m)	17,025	4.8	2.62	44,642	21.54%
BC 3 (30–40 m)	1546	5.2	3.26	5047	2.43%
BC 4 (40–50 m)	312	5.8	4.36	1360	0.66%
Total	94,992		2.18	207,281	100.00%

Source: Own calculation.

Figure 7 depicts the expected annual production for all grid cells in Berlin.

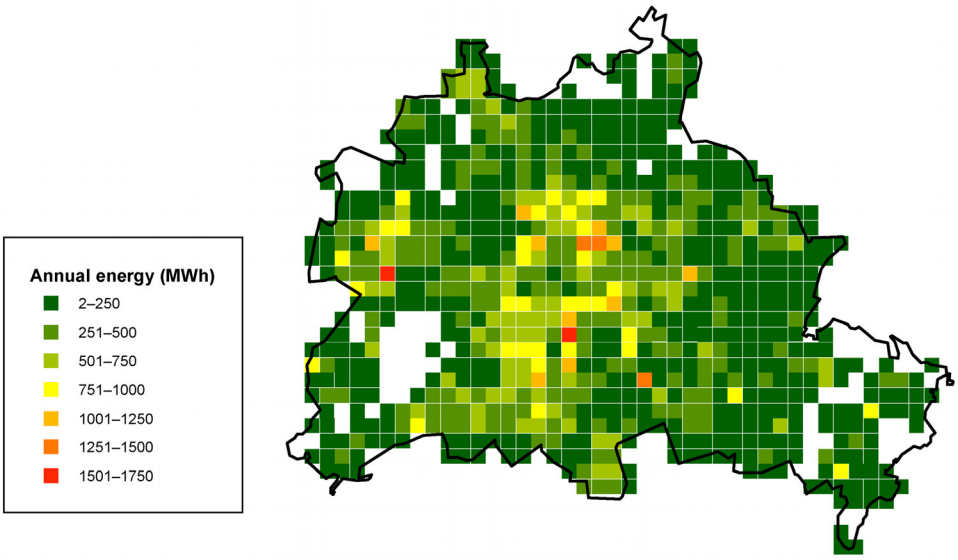

Figure 7. Expected annual energy production per grid cell (1 km^2) in Berlin. Source: Own calculation.

The basis for these calculations is the average wind speed in each grid cell extrapolated to the hub height of a turbine installed on a building, but the main driver for the results is the number of buildings per cell (Figure 5). Hence, it is not surprising that annual production is rather low in the outskirts of Berlin. High values are achieved in the center of Berlin, its southern districts, and in the west (Spandau) where there are more buildings. Two cells show an expected annual production of over 1500 MWh. This is due to the unusual high number of buildings in these cells. The aforementioned grid cell with the highest number of buildings (Horseshoe Estate) does not lead to maximal production because of the low height of most of the buildings.

Through an installation of one turbine on each building in Berlin that is at least 10 m high and has a roof surface of at least 2 m^2, only about 5% of the electricity consumption by households in Berlin could be covered. To get an impression of the related CO_2 reduction, we compare it with the primary energy consumption by lignite, which is the energy source with the highest CO_2 emissions. In 2017, 1680 GWh of the primary energy consumption were produced by lignite, leading to CO_2 emissions of 653,000 tons [45]. With 207 GWh of energy produced from the SWT, 12.34% of the energy drawn from lignite production could

be replaced. This reduction of lignite consumption would be replaced by CO_2-neutral wind energy, hence saving 80,568 tons of CO_2 emissions, which corresponds to 80,568 allowances from the EU Emission Trading Scheme. To put the expected yearly energy production of 207 GWh in Scenario 1 further into context, it can be compared with the expected production of large wind turbines and photovoltaic. The value 207 GWh corresponds to the expected annual energy production of a wind farm with 45 turbines of type Enercon E-82 (rated capacity of 2300 kW) or a wind farm with 27 turbines of type Vestas V112 (rated capacity of 3000 kW), located near Berlin. If this energy were produced offshore, it would require about 4 to 5 of the currently most powerful offshore turbines, GE 12X with a rated capacity of 12 MW.

Although the installation of one turbine on more than 90,000 buildings in Berlin seems like a large effort, the resulting energy production and CO_2 emission reduction are rather modest. However, this corresponds to only about 15% of the buildings in Berlin and, compared to the city's 3.7 million inhabitants, to one turbine every 40 people.

The buildings used in the analysis have an average roof area of 218 m^2 and a mean perimeter of 68 m. Hence, it would also be possible to install more than one turbine on many buildings. To allow the number of turbines per building depend on the roof area, in Scenario 2 we hypothetically install multiple turbines on a roof, based on the building's perimeter.

Whereas in Scenario 1 one turbine is assumed to be installed at the best position on the roof (marked in light red in Figure 8), in Scenario 2 the two edges with the most favorable wind conditions are used (marked in dark blue in Figure 8). Assuming a rectangular building with perimeter $P = 2a + 2b$, this means that a length of $a + b$ could be used for every building, which corresponds to half of the perimeter. Moreover, we consider a safety distance of 5 m between the turbines. With these conditions, we can calculate the potential of multiple turbines per building (Scenario 2).

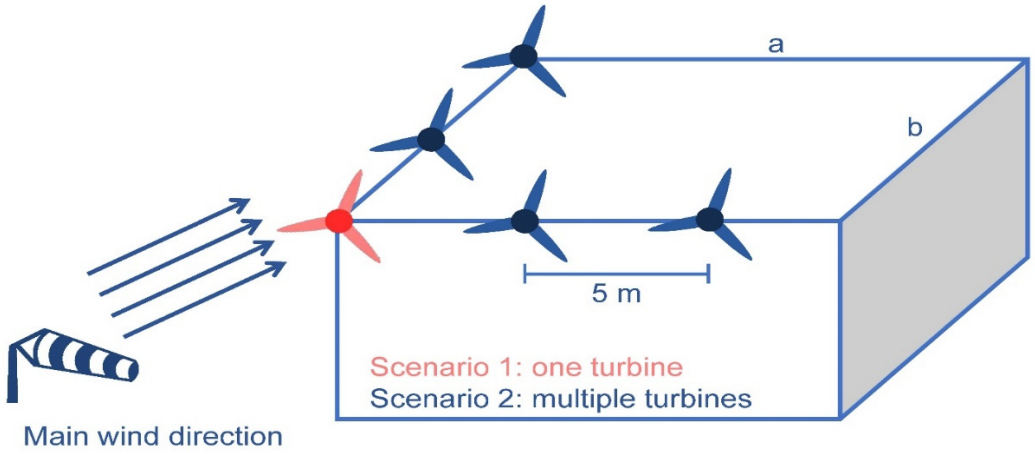

Figure 8. Illustration of Scenario 1 and Scenario 2 with a and b being the side lengths of the rectangular building. Source: Own representation.

Scenario 2 would lead to an installation of 697,596 turbines in Berlin and to an energy production of 1,535 GWh, which covers almost 37% of households' electricity consumption in 2017 (see Table 4, Scenario 2) [45]. In addition, 91% of the lignite used for primary energy consumption in 2017 could be replaced, thereby reducing CO_2 emissions by 596,758 tons [45].

Table 4 compares the energy output of both scenarios with total electricity consumption by households in Berlin in 2017 (4184 GWh) [45].

Table 4. Comparison of expected annual energy production with electricity consumption by households, lignite consumption, and CO_2 emissions in 2017.

	Scenario 1 (One Turbine Per Building)	Scenario 2 (Multiple Turbines Per Building)
Number of turbines	94,992	697,596
Annual energy production (MWh)	207,281	1,535,051
Share of covered electricity consumption by households	4.95%	36.69%
Reduction of lignite-related CO_2 emissions (tons)	80,581	596,758
Reduction of lignite-related CO_2 emissions (percentage)	12.34%	91.39%

Source: Own calculation and AfS (2019) [45].

4.1.2. Sensitivity Analysis

Potential wake effects, coming from higher buildings and nearby turbines, add uncertainty when estimating the wind energy potential [46,47]. To obtain an impression of the severeness, we account for wake effects of buildings and turbines in the following way: for each of the 94,992 turbines from Scenario 1, a building wake effect is expected if at least one building stands within 100 m in direction west-southwest (the most common wind directions from Figure 3) that is higher than the turbine location. This applies to only 4.5% of the turbine since there are not many high buildings in Berlin and their sizes do not differ much. For these turbines, we reduce the expected annual production by 90% (building wake effect). Moreover, we expect a wake effect if at least one turbine is installed within 30 m (corresponding to about 10 diameters of our exemplary turbine) in direction west-southwest at the same height, including variations of 5 m above or below (turbine wake effect). This turbine wake effect applies to 25.51% of the turbines from Scenario 1.

The literature on turbine wake effects is scarce for small wind turbines. For small horizontal wind turbines, Kenny et al. (2013) [48] observe a 25% reduction of the power output 5.7 diameters downwind. For off-shore turbines, Barthelmie et al. (2009) [49] find a reduction of 40% if turbines are exactly aligned towards the wind direction seven rotor diameters downwind. For VAWTs, Razaeiha et al. (2020) [50] apply a reduction of 12%, which is derived from a large number of simulations with varying distances between 1.25 and 10 turbine diameters. The work of Razaeiha et al. (2020) [50] is closest to our application, such that we also opt for a reduction of the expected yearly production by 12% (turbine wake effect). Considering the wake effects of both buildings and turbines, the total annual energy production in Scenario 1 reduces by 7% to 193 GWh (see Table 5). We continue the sensitivity analysis by assuming a more conservative reduction through the turbine wake effect, namely 50%, while keeping the building wake effect at a 90% reduction. The total annual energy production in Scenario 1 would then amount to 174 GWh (−16%).

Table 5. Sensitivity analysis of the results with respect to wake effects.

	Scenario 1 (One Turbine Per Building)		Scenario 2 (Multiple Turbines Per Building)	
Annual energy production (MWh)	207,281		1,535,051	
- with wake effect of buildings (−90%) and turbines (−12%)	193,317	*(−7%)*	1,059,825	*(−31%)*
- with wake effect of buildings (−90%) and turbines (−50%)	173,792	*(–16%)*	436,085	*(−72%)*

Source: Own calculation.

The turbine wake effect becomes more severe in Scenario 2 with multiple turbines per building. Although we do not specify the exact location of the turbines on the roof, we assume that they are optimally aligned according to the main wind directions. From Figure 8, which illustrates the turbine alignment exemplarily for a rectangular roof, we

can derive an assessment of the wake effect: The first turbine (in red) is not affected by the other turbines on the building, the two turbines in the next row are affected by one turbine, the two turbines behind are affected by two turbines and so on. This allows a calculation of the reduction in dependence of the number of turbines. Assuming again a reduction by one turbine of 12% or 50%, the total annual energy production reduces to 1060 GWh (−31%) or 436 GWh (−72%), respectively. This illustrates the importance of correctly capturing the turbine wake effect coefficient.

As mentioned in Section 2.1, we considered the roughness length z_0 to be 2 since Berlin consists of suburban areas (corresponding to z_0 = 1.5) and city center areas (corresponding to $z_0 = 3$). To explore the sensitivity of our results to this parameter, we rerun the analysis from Scenario 1 assuming $z_0 = 1.5$ or $z_0 = 3$. It turns out that the expected yearly energy production of 207 GWh would change to 184 GWh (−11%) and 248 GWh (+20%), respectively.

4.2. Household-Level

Besides the overall energy production of reference turbines at the city-level, it is especially interesting to break down the simulation results at the household- and resident-level.

Each inhabitant in Berlin consumed an annual average of 1.1 MWh of electricity in 2017 [45]. Figure 9 compares this per capita consumption to the average annual production outcome of one turbine under the TRY 2015 in the different building categories. It can be observed that one turbine on a building of average height exceeds the annual electricity demand of one resident in each BC. In fact, it provides enough energy to meet the average private electricity demand of almost four residents for buildings above 40 m in height (BC 4). However, since one building, especially one of greater height, is very likely to accommodate more than four people, the production of a single turbine is presumably not enough to meet the electricity demand of a whole apartment building. Still, the installation of one turbine on a building with 10 m–20 m height could supply approximately the annual electricity consumption of two people.

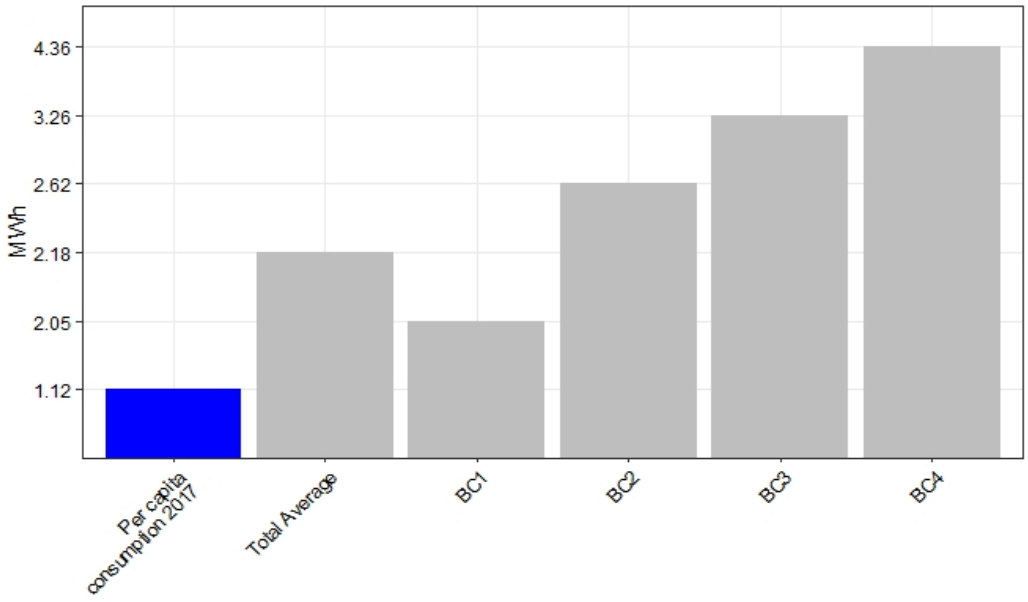

Figure 9. Average annual energy production for one reference turbine versus per capita consumption. Source: Own calculation.

4.3. Economic Evaluation

The LCOE of the rooftop installation of a single turbine is assessed for an average building in each BC. The specific input values for the LCOE calculation according to

Equation (3) are summarized in Table 6. For further information on the input values, see Appendix B.

Table 6. Input data to the LCOE calculation.

Inputs to LCOE Calculation	Value
Initial investment C_0	EUR 4416
Purchase costs C_P	EUR 3840
Installation costs C_I	EUR 576
Annual Outflows o_t	
Maintenance costs $o_{M,t}$	EUR 77
Debt service $o_{D,t}$	varies with t
Interest rate for debt	1.44%
Discount rate r_d	
100% loan financed, $r_{d,\,debt}$	1.43%
100% equity financed, $r_{d,\,equity}$	/
Low CoE	4%
Medium CoE	5.5%
High CoE	7%

Source: Own representation; details are provided in Appendix B.

From the LCOE calculation in Figure 10 it can be observed that debt-financing yields lower LCOE than equity-financing in all BC, even though debt-financing involves higher annual outflows through debt service. In this example, the relatively higher discount rates of equity as compared to the discount rate of debt were a more important driver for the LCOE than the higher annual out-flows in case of debt-financing. As expected, equity-financing with high CoE, yields higher LCOE. However, the CoE do not make a difference regarding the general profitability of the investment. The latter can be derived by comparing the LCOE to the sales price of electricity, i.e., the feed-in tariff, or to the opportunity costs of self-consumption, i.e., the current electricity price (see dotted lines in Figure 10). For the investment to be profitable, the tariff must be at least as high as the LCOE.

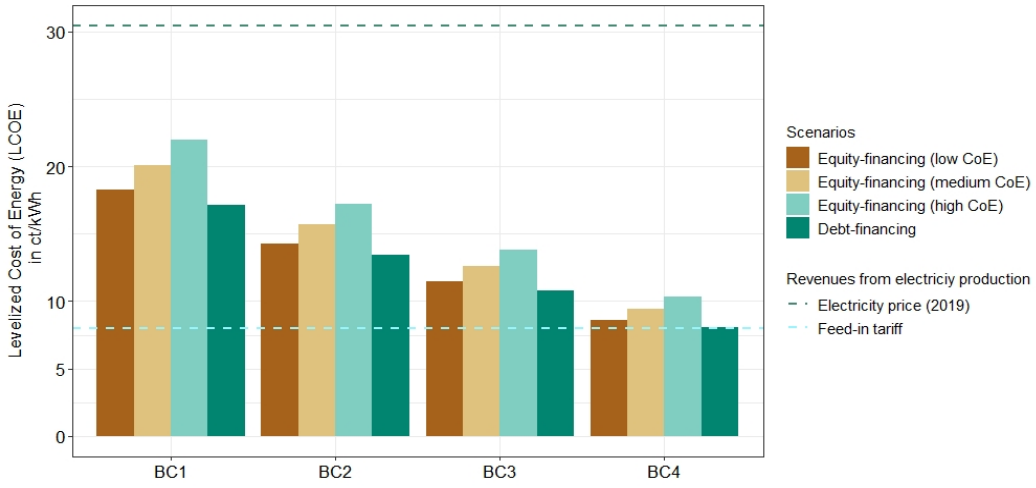

Figure 10. LCOE analysis under different scenarios. Source: Own calculation.

The feed-in tariff that is granted under the German Renewable Energy Act (EEG), namely 8.03 ct/kWh, does barely cover the LCOE in BC 4 when debt-financing is applied [51]. In all other cases, selling the self-produced electricity to the grid provider under this subsidized tariff will lead to losses. If the produced electricity is self-consumed, however, the "prosumer" saves the electricity retail price which she pays if she buys electricity from the grid provider. Self-consumption does not only cover the LCOE but generates profits with each generated kWh in all BCs.

5. Discussion

While the potential of approximately 95,000 SWT seems rather modest (Scenario 1), it involves a substantial potential from a household perspective, even at lower building heights, as we show in the economic evaluation. We find self-consumption of electricity to be the financially better choice compared to selling the electricity to the grid provider, which is in line with research results from other authors [52–54]. It might especially be interesting for owners of apartment buildings with large rooftops to construct several turbines and self-consume the produced electricity. Other authors find SWT only to be profitable if the area has a low building density and therefore has less obstacles to steady wind flows [10,55]. We agree that SWT, at least at their current state of efficiency, are unlikely to yield a profitable investment under the current feed-in tariff in the German Renewable Energy Act (EEG), especially urban areas [10,11]. The current subsidized feed-in tariff is unlikely to increase any time soon. The last amendment of the EEG focused on the opening of the market for self-produced (wind-) energy towards less subsidies and more competition [51]. It appears to be more likely that subsidized feed-in tariffs for SWT will be removed in future amendments of the EEG [56]. Our economic evaluation serves as an illustration of simple investment scenarios. Its results are sensitive to changes of the financing structure, the initial investment, the discount rate, or other assumptions made during its calculation, such as the consideration of taxes.

The installation of (several) SWT on suitable buildings could be profitable for many building owners, and therefore contribute to the energy transition of cities. Whereas it is beneficial for individuals, doing this at a large scale would require a more detailed analysis about the consequences, for instance, aesthetic perception, shadowing, or costs for maintaining the grid. In general, exploring the community and political acceptance of SWT and/or photovoltaic would be important (see Mamkhezri et al., 2020 [57] and Harold et al., 2021 [58]).

Regional electricity price volatility could increase if a large part of electricity is supplied by renewables [59–63]. While spot price volatility might increase, the average electricity price is found to decrease with a high share of renewables in the energy mix [59–63]. The average decrease of spot prices might also lead to a substantial drop in market value of renewables, decreasing research incentives for producers. Policy intervention might therefore become even more important in the future [63]. The internalization of environmental costs of fossil fuels and price caps that shield consumers from volatile electricity prices could assure a long-run market equilibrium with a very high share of renewable energies [63].

Estimates about the solar potential of Berlin assess the annual energy production by photovoltaic between 2900 and 5900 GWh [64] and hence more than twice the estimated energy production in Scenario 2. This highlights that the solar potential is much higher and that SWT should rather be considered as a complement to photovoltaic in urban areas.

6. Conclusions

This paper presents a framework for a straightforward assessment of the potential and profitability of urban wind energy production. An exemplary turbine was chosen to simulate wind energy potential in Berlin based on a complete dataset of buildings in Berlin and hourly wind speeds at a 1 km^2 resolution for a test reference year. One of our output datasets is publicly available upon request. It contains all buildings in Berlin, including their coordinates, roof-surface, building height, and a unique ID.

Future research could address the effect of changing wind directions on energy production, the exact locations of turbines and the specific extent of individual buildings. The latter could be covered by using a more detailed building dataset, such as Level of Detail 2. Another interesting extension of this work is the practical validation with real measurements, such as a prototype SWT. Regarding the economic evaluation, a direct comparison of the hourly produced energy with the hourly consumption would be interesting. For this purpose, however, more detailed real wind speeds instead of average hourly wind speeds

would be necessary, as well as detailed hourly consumption data. One might also consider possibilities for the storage of self-produced electricity. Whereas we focused mainly on SWT in this study, other renewable energy sources might be more beneficial to be used in Berlin. Future studies might consider combining two sources, such as photovoltaic and wind energy, and investigate on a deeper level how they can complement each other.

For policy makers, our analysis is a starting point in the search for the right energy mix. It demonstrates the importance of carefully investigating the advantages and disadvantages of each energy type with respect to the local climatic conditions. Policy makers should be aware that the feed-in tariff for selling self-produced electricity of SWT to the grid provider is crucial for the future role of SWT in the renewable energy mix. Not all the produced electricity can be consumed on site and battery capacity might not be sufficient to balance production variance. If there were higher subsidies on feed-in tariffs, demand for SWT would increase, which makes technology investments for manufacturers more attractive.

Author Contributions: Conceptualization, A.W.; methodology, A.W. and M.R.; software, A.W..; validation, A.W., M.R. and Z.S.; formal analysis, A.W. and M.R.; investigation, A.W.; resources, does not apply; data curation, A.W.; writing—original draft preparation, A.W.; writing—review and editing, A.W., M.R. and Z.S.; visualization, A.W. and M.R.; supervision, M.R. and Z.S.; project administration, does not apply; funding acquisition, does not apply. All authors have read and agreed to the published version of the manuscript.

Funding: This research received no external funding.

Data Availability Statement: All input data to our analysis is (upon request) publicly available. The input wind data (Test reference year) is provided by Deutscher Wetterdienst and freely available. It can be found here: https://www.dwd.de/DE/leistungen/testreferenzjahre/testreferenzjahre.html (last accessed: 31 August 2021, 11:28). The input building data is available upon request (from non-private institutions) in CityGML format: http://www.adv-online.de/AdV-Produkte/Weitere-Produkte/3D-Gebaeudemodelle-LoD/ (last accessed: 31 August 2021, 11:28). A major part of the contribution of this paper is the processing of the building data. We added coordinates and roof-surfaces for each building and assigned a unique code to each—it is available upon request to the corresponding author.

Conflicts of Interest: The authors declare no conflict of interest.

Appendix A. Building Dataset—Transformation Process

This appendix provides more detail on the preparation and specifications of the building dataset. Objects in the 3D-Building Model are divided into "Buildings" (B) and "Building Parts" (BP), whereby the BP are subordinated to the B. In the graphical representation, however, the B do not comprise the shape of the building entirely nor do they necessarily represent a central point of the whole building. Rather, B seem to constitute, at least in the graphical representation of the dataset, as BP themselves.

For each B-object, the "measured height" is specified, which is defined as the "*height of the building from the difference between the height of the roof and the ground level*" [65]. This altitude indication is used in the analysis to define the height of the building.

Due to the Level of Detail 1 (LoD1) representation, there might be parts of the buildings that are actually higher than the average height of the building block, which is provided by the LoD1 representation, and hence would provide better wind conditions for a turbine. In addition, there might be buildings considered in this analysis that do not allow for the installation of a turbine due to roof shapes or other obstacles. This simplified assessment of buildings and their heights is nevertheless a good approximation to assess the overall potential for wind energy production in Berlin.

To assign each building to its respective grid cell, it is necessary that each building has a unique coordinate. For that purpose, a central point is computed for each B-object. BP do not enter in this process because the "measured height" variable is only available for the whole building, namely the B-object. Therefore, the computed central point does not necessarily represent the center of the whole building, but instead the center of the

B-object. This slight imprecision, however, will be mostly offset during the analysis as each building is assigned to grid cell-specific wind data from the TRY dataset. Figure A1 gives an insight into the accuracy of the center points calculated for the B-objects related to the actual position of the building. It shows the B- and BP-objects (white), together with the calculated center points of the B-objects (red).

Figure A1. B- and BP-objects with center points of B-objects. Source: Own calculation and representation based on Senatsverwaltung für Stadtentwicklung und Wohnen Berlin, 2015 [43].

Appendix B. Economic Evaluation

This appendix provides more detail on the input values for LCOE calculation. The appendix provides more detail on the input values for LCOE calculation. The manufacturer of the reference turbine Skyline SL-30 does not provide prices on their website, wherefore it was drawn from Bortolini et al. (2014) [11]. Installation costs C_I of the reference turbine depend on purchase costs C_P, as do annual maintenance costs $o_{M,t}$. In other studies, annual operation and maintenance costs are commonly considered to be 2% of the turbine purchasing price, such that the maintenance costs o_M account for the same amount in every period.

Annual outflows o_t and the discount rate r_d depend on the selected financing method. This work considers the possibilities of complete equity-financing and complete debt-financing. If complete equity-financing is chosen, annual outflows consist of time independent maintenance costs as a share of the purchase price. The annual costs of equity, which serve as a discount factor for equity capital, are the expected returns to project sponsors [33]. Egli et al. (2018) [33] studied the cost of capital for renewable energy projects in Germany, including cost of equity, of 78 wind onshore projects between 2000 and 2017. They found the lower bound of cost of equity in 2017 to be approximately 4%, without taxes considered. The average equity costs in 2017 were 5.4%, the upper bound lay at around 7%. This study comprises a sensitivity analysis, considering three different discount rates of equity, namely (a) 4%, (b) 5.5% and (c) 7%.

If complete debt-financing is chosen, annual outflows consist of time independent maintenance costs, interest payments, and repayments of debt to the creditor. For the cost of debt in 2017 Egli et al. (2018) [33] found the lower bound to be approximately 1%, the average to be 1.6% and the upper bound of cost of debt to lay around 2% for wind onshore projects. These limits correspond to the interest rate the German development bank KfW offers in its current credit program for renewable energy investments [66]. The annual interest rate for a good degree of creditworthiness (resulting in price category "B", which assumes an annual default probability between 0.4 to 1.2% and value of collateral securities of at least 70% of the loan), 20 years of maturity, a fixed interest rate, and a 3-year

grace period, is 1.43%, which corresponds to an effective interest rate of 1.44% [66,67]. This exemplary effective interest rate of KfW will be used as the discount factor for debt capital. The annual interest rate is used to calculate annual interest payments.

The cash inflows in BC j account for the same amount in each period t. The reason for this is that electricity production is calculated through the TRY 2015 wind dataset, which contains average wind observations over several years. LCOEs are compared to potential sources of revenue from electricity generation to determine the profitability of the investment. The potential sources of revenues, considered in this analysis are as follows:

1. The produced energy is sold to the grid provider:

In this case, the electricity price is defined as the feed-in tariff that is received when the produced electricity is fed into the grid. This feed-in tariff is guaranteed under the German EEG regime, a legislation that was introduced in 2000 and amended last in 2017. Very small turbines with capacities at 50 kW and below receive a subsidy of 8.03 ct./kWh during the whole remuneration period of 20 years [68,69].

2. The produced energy is self-consumed:

Here, the electricity price is defined as the electricity retail price. The average electricity retail price for German households in the beginning of 2019 will be used for comparison, which amounts to 30.43 ct./kWh [70].

References

1. International Energy Agency. Global Energy Review 2021. Assessing the Effects of Economic Recoveries on Global Energy Demand and CO2 Emissions in 2021. Available online: https://www.iea.org/reports/global-energy-review-2021/renewables (accessed on 18 February 2021).
2. International Energy Agency. World Energy Balances: Overview. Available online: https://www.iea.org/reports/world-energy-balances-overview/world (accessed on 18 August 2021).
3. Busu, M.; Nedelcu, A.C. Analyzing the renewable energy and CO_2 emission levels nexus at an EU level: A panel data regression approach. *Processes* **2021**, *9*, 130. [CrossRef]
4. Azam, A.; Rafiq, M.; Shafique, M.; Zhang, H.; Yuan, J. Analyzing the effect of natural gas, nuclear energy and renewable energy on GDP and carbon emissions: A multi-variate panel data analysis. *Energy* **2021**, *219*, 119592. [CrossRef]
5. United Nations. The Paris Agreement. 2015. Available online: http://unfccc.int/files/essential_background/convention/application/pdf/english_paris_agreement.pdf (accessed on 15 July 2021).
6. European Commission. Delivering the European Green Deal. Available online: https://ec.europa.eu/info/strategy/priorities-2019--2024/european-green-deal/delivering-european-green-deal_en (accessed on 22 August 2021).
7. Baltagi, B.H.; Bresson, G.; Etienne, J.-M. Carbon dioxide emissions and economic activities: A mean field variational bayes semiparametric panel data model with random coefficients. *Ann. Econ. Stat.* **2019**, *134*, 43–77. [CrossRef]
8. Hyams, M.A. Wind energy in the built environment. In *Metropolitan Sustainability: Understanding and Improving the Urban Environment*; Zeman, F., Ed.; Woodhead Pub. Ltd.: Cambridge, UK, 2012; pp. 457–499. ISBN 9780857090461.
9. Scholten, D.; Criekemans, D.; van de Graaf, T. An energy transition amidst great power rivalry. *J. Int. Aff.* **2019**, *73*, 195–204.
10. Grieser, B.; Sunak, Y.; Madlener, R. Economics of small wind turbines in urban settings: An empirical investigation for Germany. *Renew. Energy* **2015**, *78*, 334–350. [CrossRef]
11. Bortolini, M.; Gamberi, M.; Graziani, A.; Manzini, R.; Pilati, F. Performance and viability analysis of small wind turbines in the European Union. *Renew. Energy* **2014**, *62*, 629–639. [CrossRef]
12. KC, A.; Whale, J.; Urmee, T. Urban wind conditions and small wind turbines in the built environment: A review. *Renew. Energy* **2019**, *131*, 268–283. [CrossRef]
13. V, Sri Ragunath and Pandey, Jitendra K and Mondal, Amit Kumar and Karn, Ashish, Electricity Generation from Wind Turbines at Low Wind Velocities: A Review. 2019. Available online: https://ssrn.com/abstract=3372736 (accessed on 31 August 2021).
14. Chong, W.T.; Pan, K.C.; Poh, S.C.; Fazlizan, A.; Oon, C.S.; Badarudin, A.; Nik-Ghazali, N. Performance investigation of a power augmented vertical axis wind turbine for urban high-rise application. *Renew. Energy* **2013**, *51*, 388–397. [CrossRef]
15. Wen, W.T.; Palanichamy, C.; Ramasamy, G. Small wind turbines as partial solution for energy sustainability in Malaysia. *Int. J. Energy Econ. Policy* **2019**, *9*, 257–266.
16. Arteaga-López, E.; Angeles-Camacho, C. Innovative virtual computational domain based on wind rose diagrams for micrositing small wind turbines. *Energy* **2020**, *220*, 119701. [CrossRef]
17. Ishugah, T.; Li, Y.; Wang, R.; Kiplagat, J. Advances in wind energy resource exploitation in urban environment: A review. *Renew. Sustain. Energy Rev.* **2014**, *37*, 613–626. [CrossRef]
18. Twele, J. *Empfehlungen zum Einsatz kleiner Windenergieanlagen im urbanen Raum*; Reiner Lemoine Institute: Berlin, Germany, 2015.

19. Stathopoulos, T.; Alrawashdeh, H.; Al-Quraan, A.; Blocken, B.; Dilimulati, A.; Parashivoiu, M.; Pilay, P. Urban wind energy: Some views on potential and challenges. *J. Wind Eng. Ind. Aerodyn.* **2018**, *179*, 146–157. [CrossRef]
20. Battisti, L.; Benini, E.; Brighenti, A.; Dell'Anna, S.; Castelli, M.R. Small wind turbine effectiveness in the urban environment. *Renew. Energy* **2018**, *129*, 102–113. [CrossRef]
21. Hupfer, P.; Chmielewski, F.-M. (Eds.) *Das Klima von Berlin*; Akademie-Verlag: Berlin, Germany, 1990; ISBN 3055006305.
22. Hupfer, P.; Becker, P.; Börngen, M. *20,000 Jahre Berliner Luft: Klimaschwankungen im Berliner Raum*; Gutenbergplatz: Leipzig, Germany, 2013; ISBN 9783937219622.
23. Gualtieri, G.; Secci, S. Methods to extrapolate wind resource to the turbine hub height based on power law: A 1-h wind speed vs. Weibull distribution extrapolation comparison. *Renew. Energy* **2012**, *43*, 183–200. [CrossRef]
24. Gualtieri, G.; Secci, S. Comparing methods to calculate atmospheric stability-dependent wind speed profiles: A case study on coastal location. *Renew. Energy* **2011**, *36*, 2189–2204. [CrossRef]
25. Counihan, J. Adiabatic atmospheric boundary layers: A review and analysis of data from the period 1880–1972. *Atmos. Environ.* **1975**, *9*, 871–905. [CrossRef]
26. Manwell, J.F.; McGowan, J.G.; Rogers, A.L. *Wind Energy Explained*; John Wiley & Sons, Ltd.: Chichester, UK, 2009; ISBN 9781119994367.
27. Elnaggar, M.; Edwan, E.; Ritter, M. Wind energy potential of Gaza using small wind turbines: A feasibility study. *Energies* **2017**, *10*, 1229. [CrossRef]
28. Irwin, J.S. A theoretical variation of the wind profile power-law exponent as a function of surface roughness and stability. *Atmos. Environ.* **1979**, *13*, 191–194. [CrossRef]
29. Cleveland, C.J.; Morris, C.G. *Dictionary of Energy*, 2nd ed.; Elsevier: Amsterdam, The Netherlands, 2015; ISBN 0080968120.
30. Smedman-Högström, A.-S.; Höström, U. A practical method for determining wind frequency distributions for the lowest 200 m from routine meteorological data. *J. Appl. Meteorol.* **1978**, *17*, 942–954. [CrossRef]
31. WMO. *Guide to Meteorological Instruments and Methods of Observation*; (WMO-No. 8); WMO: Geneva, Switzerland, 2018; ISBN 978-92-63-10008-5.
32. Sunderland, K.M.; Narayana, M.; Putrus, G.; Conlon, M.F.; McDonald, S. The cost of energy associated with micro wind generation: International case studies of rural and urban installations. *Energy* **2016**, *109*, 818–829. [CrossRef]
33. Egli, F.; Steffen, B.; Schmidt, T.S. A dynamic analysis of financing conditions for renewable energy technologies. *Nat. Energy* **2018**, *3*, 1084–1092. [CrossRef]
34. Steffen, B. Estimating the cost of capital for renewable energy projects. *Energy Econ.* **2020**, *88*, 104783. [CrossRef]
35. Ragheb, M. *Economics of Wind Power Generation*; Elsevier: Amsterdam, The Netherlands, 2017; pp. 537–555. [CrossRef]
36. MWEA. Domestic Roof-Mounted Wind Turbines: The Current State of the Art. 2005. Available online: https://www.solarcollect.co.uk/downloads/domturbinerep.pdf (accessed on 31 August 2021).
37. Amt für Statistik Berlin-Brandenburg. *Kleine Statistik Berlin 2018*; Amt für Statistik Berlin-Brandenburg: Potsdam, Germany, 2018; Available online: https://www.statistik-berlin-brandenburg.de/kleine-statistiken-6bffdf63bfa0f54c (accessed on 31 August 2021).
38. BauO Bln. Bauordnung für Berlin. 2011. Available online: http://www.bauordnungen.de/Berlin.pdf (accessed on 31 August 2021).
39. Deutscher Wetterdienst (DWD). Bundesamt für Bauwesen und Raumordnung. Testreferenzjahre (TRY). Available online: https://www.dwd.de/DE/leistungen/testreferenzjahre/testreferenzjahre.html (accessed on 15 July 2021).
40. Krähenmann, S.; Walter, A.; Brienen, S.; Imbery, F.; Matzarakis, A. High-resolution grids of hourly meteorological variables for Germany. *Theor. Appl. Clim.* **2016**, *131*, 899–926. [CrossRef]
41. Lun, I.Y.; Lam, J.C. A study of Weibull parameters using long-term wind observations. *Renew. Energy* **2000**, *20*, 145–153. [CrossRef]
42. Deutscher Wetterdienst. Hourly Historical Wind Data. Available online: https://opendata.dwd.de/climate_environment/CDC/observations_germany/climate/hourly/wind/ (accessed on 15 July 2021).
43. Senatsverwaltung für Stadtentwicklung und Wohnen Berlin. 3D-Gebäudemodelle im Level of Detail 1 (LoD 1) [Atom]. Available online: https://daten.berlin.de/datensaetze/3d-gebäudemodelle-im-level-detail-1-lod-1-atom (accessed on 31 August 2021).
44. En-eco. Skyline sl-30, Technial Specifications: 3 kW Vertical Axis Wind Turbine. Available online: https://www.solarenergypoint.it/catalogo/schede_tecniche/eolico/en-eco/en-eco_skyline_3_kw_scheda_tecnica.pdf (accessed on 31 August 2021).
45. AfS. Energie- und CO_2-Bilanz in Berlin 2017: Statistischer Bericht E IV 4-j/17. 2019. Available online: https://www.statistik-berlin-brandenburg.de/publikationen/stat_berichte/2019/SB_E04-04-00_2017j01_BE.pdf (accessed on 31 August 2021).
46. Magnusson, M.; Smedman, A.-S. Air flow behind wind turbines. *J. Wind. Eng. Ind. Aerodyn.* **1999**, *80*, 169–189. [CrossRef]
47. Ritter, M.; Deckert, L. Site assessment, turbine selection, and local feed-in tariffs through the wind energy index. *Appl. Energy* **2017**, *185*, 1087–1099. [CrossRef]
48. Kenny, W.; Corscadden, K.; Lubitz, W.D.; Thomson, A.; McCabe, J. Investigation of wake effects on the energy production of small wind turbines. *Wind. Eng.* **2013**, *37*, 151–163. [CrossRef]
49. Barthelmie, R.J.; Hansen, K.; Frandsen, S.T.; Rathmann, O.; Schepers, J.G.; Schlez, W.; Phillips, J.; Rados, K.; Zervos, A.; Politis, E.S.; et al. Modelling and measuring flow and wind turbine wakes in large wind farms offshore. *Wind. Energy* **2009**, *12*, 431–444. [CrossRef]

50. Rezaeiha, A.; Montazeri, H.; Blocken, B. A framework for preliminary large-scale urban wind energy potential assessment: Roof-mounted wind turbines. *Energy Convers. Manag.* **2020**, *214*, 112770. [CrossRef]
51. EEG. Gesetz für den Vorrang Erneuerbarer Energien (Erneuerbare-Energien-Gesetz—EEG 2000). 2000. Available online: https://www.bgbl.de (accessed on 31 August 2021).
52. Kleinwindanlagen. *Handbuch der Technik, Genehmigung und Wirtschaftlichkeit Kleiner Windräder*; Franken, M., Ed.; Bundesverband Wind Energie: Berlin, Germany, 2013; ISBN 9783942579179.
53. Jüttemann, P. Wichtige Themen zu Kleinwindkraftanlagen. Available online: https://www.klein-windkraftanlagen.com/ (accessed on 17 February 2020).
54. Feddersen, C.; Franken, M.; Jensen, D.; Jüttemann, P.; Lehmkuhl, V.; Rentzing, S.; Weller, K. *Energiewende selber machen*; Bundesverband Windenergie: Berlin, Germany, 2015; ISBN 978-3942579278.
55. Pitteloud, J.-D.; Gsänger, S. Small Wind World Report 2017: Summary. 2017. Available online: http://www.wwindea.org/download/SWWR2017-SUMMARY(2).pdf (accessed on 15 July 2021).
56. BMWi. EEG-Vergütung und Kapazitätszuweisung. Available online: https://www.erneuerbare-energien.de/EE/Navigation/DE/Technologien/Windenergie-auf-See/Finanzierung/EEG-Verguetung/eeg-verguetung.htm (accessed on 31 August 2021).
57. Mamkhezri, J.; Thacher, J.A.; Chermak, J.M. Consumer preferences for solar energy: A choice experiment study. *Energy J.* **2020**, *41*. [CrossRef]
58. Harold, J.; Bertsch, V.; Lawrence, T.; Hall, M. Drivers of people's preferences for spatial proximity to energy infrastructure technologies: A cross-country analysis. *Energy J.* **2021**, *42*. [CrossRef]
59. Kolb, S.; Dillig, M.; Plankenbühler, T.; Karl, J. The impact of renewables on electricity prices in Germany—An update for the years 2014–2018. *Renew. Sustain. Energy Rev.* **2020**, *134*, 110307. [CrossRef]
60. Cludius, J.; Hermann, H.; Matthes, F.C.; Graichen, V. The merit order effect of wind and photovoltaic electricity generation in Germany 2008–2016: Estimation and distributional implications. *Energy Econ.* **2014**, *44*, 302–313. [CrossRef]
61. Rai, A.; Nunn, O. On the impact of increasing penetration of variable renewables on electricity spot price extremes in Australia. *Econ. Anal. Policy* **2020**, *67*, 67–86. [CrossRef] [PubMed]
62. Dillig, M.; Jung, M.; Karl, J. The impact of renewables on electricity prices in Germany—An estimation based on historic spot prices in the years 2011–2013. *Renew. Sustain. Energy Rev.* **2016**, *57*, 7–15. [CrossRef]
63. Helm, C.; Mier, M. On the efficient market diffusion of intermittent renewable energies. *Energy Econ.* **2019**, *80*, 812–830. [CrossRef]
64. Bergner, J.; Siegel, B.; Quaschning, V. *Das Berliner Solarpotenzial: Kurzstudie zur Verteilung des solaren Dachflächenpoten-zials im Berliner Gebäudebestand*; Hochschule für Technik und Wirtschaft Berlin: Berlin, Germany, 2013.
65. LDBV. Data Format Specification of the Official 3D Building Model LoD1 of Germany (LoD1-DE): For the Data Distribution from the Data Stock of the Central Office for House Coordinates and Building Polygons (ZSHH). Available online: http://mobile.adv-online.de/AdV-Produkte/Standards-und-Produktblaetter/ZSHH/ (accessed on 15 July 2021).
66. KfW. Merkblatt. Erneuerbare Energien. KfW-Programm Erneuerbare Energien "Standard". Available online: https://www.kfw.de/s/deiDsnB (accessed on 15 July 2021).
67. KfW. Konditionenübersicht für Endkreditnehmer. KfW—Programm Erneuerbare Energien—Pro-grammteil "Standard". Available online: https://www.kfw-formularsammlung.de/KonditionenanzeigerINet/KonditionenAnzeiger?ProgrammNameNr=270 (accessed on 15 July 2021).
68. EEG. Gesetz für den Ausbau erneuerbarer Energien (Erneuerbare-Energien-Gesetz—EEG 2017). 2017. Available online: https://www.gesetze-im-internet.de/eeg_2014/EEG_2017.pdf (accessed on 31 August 2021).
69. SWE. Vergütungssätze Windkraftanlagen: SWE GmbH—Strom aus Windenergie. Available online: https://www.swe-windenergie.de/unternehmen/vergutungssatze-windkraftanlagen.html (accessed on 15 July 2021).
70. Bundesverband der Energie- und Wasserwirtschaft. *Strompreisanalyse Januar 2019*; Haushalte und Industrie: Berlin, Germany, 2019.